Impact of Aspect Ratio and Solar Heating on Street Conyn Air Temperature

RIZWAN AHMED MEMON*, ABDUL HAQUE TUNIO**, AND KANYA LAL***

RECEIVED ON 09.03.2010 ACCEPTED ON 03.01.2011

ABSTRACT

The results obtained from RNG (Re-Normalization Group) version of k-ε turbulence model are reported in this study. The model is adopted to elucidate the impact of different building aspect ratios (i.e., ratio of building-height-to-street-canyon-width) and solar heating on temperatures in street canyon. The validation of Navier-Stokes and energy transport equations showed that the model prediction for air-temperature and ambient wind provides reasonable accuracy. The model was applied on AR (Aspect Ratios) one to eight and surface temperature difference ($\Delta\theta_{s-a}$) of 2 -8. Notably, air-temperatures were higher in high AR street canyons in particular on the leeward side of the street canyon. Further investigation showed that the difference between the air-temperature of high and low AR street canyons (AR) was positive and high with higher $\Delta\theta_{s-a}$. Conversely, the AR become negative and low gradually with lower values of $\Delta\theta_{s-a}$. These results could be very beneficial for the city and regional planners, civil engineers and HVAC experts who design street canyons and strive for human thermal comfort with minimum possible energy requirements.

Key Words: **Surface Temperature, Turbulence, Thermal Comfort, CFD.**

1. INTRODUCTION

The inhabitants of modern cities are directly exposed to the environmental conditions in a street canyon. However, these conditions are mostly dependent on the street canyon design and other parameters and, therefore, vary considerably from area to area [1-3]. Cities are normally densely populated with higher number of people living within a small area; leading to higher AR street canyons as compared to their counterpart rural areas. It is reported that at times city average temperatures could be as high as 12°C as compared to surrounding rural areas [4]. Such higher temperatures in cities could increase energy consumption and create many associated problems [5-7]. It could particularly be important in Sindh, Pakistan where reportedly efficient control over thermal comfort and air-conditioning could reduce up-to 80% of building energy

* Assistant Professor, Department of Mechanical Engineering, Mehran University of Engineering & Technology, Jamshoro.

** Associate Professor, Institute of Petroleum and Natural Gas Engineering, Mehran University of Engineering & Technology, Jamshoro.

*** Assistant Professor, Department of Civil Engineering, Mehran University College of Engineering and Technology Khairpur Mirs.

consumption [8]. This stresses the need for understanding heating in high aspect ratio street canyons. Although there has been significant number of numerical modelling studies on determining higher heating in urban areas little work was carried out with CFD (Computational Fluid Dynamics) techniques [9-17]. Additionally, most of the studies that have used CFD techniques were focused on pollution dispersion and fluid flow [18-21]. Conversely, the studies carried out an investigation of heating have only simulated cases with lower aspect ratios [22-23]. However, relevant CFD studies show that the k-ε turbulence model has been quite successful in solving the fluid flow patterns and heating within street canyons [22, 24-27]. Furthermore, the RNG version of k-ε model appeared to be even better in solving street canyon fluid flow and heating problems [27-29]. Memon, R.A., et. al. [3] have successfully adopted the RNG k-ε turbulence model to estimate the effects of ambient wind speed (u_a) and building aspect ratio on heating within street canyon. However, the study was limited to fewer simulations and did not include the effects of surface and temperature difference ($\Delta\theta_{s-a}$). In this study four aspect ratios i.e. 1, 2, 4 and 8 and four values for $\Delta\theta_{s-a}$ i.e. 2, 4, 8 and 16K were selected. This results in 100% increase in aspect ratios and $\Delta\theta_{s-a}$ to assure that relevant change in temperature and other parameters could be analyzed; however, only one value for ambient wind speed is selected (2.5 m/s).

2. NUMERICAL MODEL

The mathematical model for this study consists of following equations for conservation of mass, momentum and energy. The model governing equations are discretized using a second-order scheme with finite volume method and are solved by CFD code Fluent 6.2.1 [30]. The detailed mathematical model is also given in Memon, R.A., et. al. [3].

$$\frac{\partial \rho}{\partial t} + \rho \frac{\partial u_j}{\partial x_j} = 0 \tag{1}$$

$$\frac{\partial \overline{u_i}}{\partial t} + \overline{u_j} \frac{\partial \overline{u_i}}{\partial x_j} = -g_i - \frac{1}{\rho} \frac{\partial \overline{p}}{\partial x_i} + \frac{v \partial^2 \overline{u_i}}{\partial x_j^2} - \frac{\partial (\overline{u_i' u_j'})}{\partial x_j} \tag{2}$$

$$\frac{\partial \overline{\theta}}{\partial t} + \frac{\overline{u_j} \partial \overline{\theta}}{\partial x_j} = \frac{v_\theta \partial^2 \overline{\theta}}{\partial x_j^2} - \frac{\partial (\overline{u_j' \theta'})}{\partial x_j} \tag{3}$$

Additional equations for turbulent kinetic energy (k) and turbulent dissipation rate (ε) were solved as given by the RNG theory to address closure problem. The empirical constants adopted to solve this model are given in Table 1.

$$\overline{u_i} \frac{\partial k}{\partial x_i} = \frac{1}{\rho} \frac{\partial}{\partial x_i} \left(\alpha_k \mu_{eff} \frac{\partial k}{\partial x_i} \right) + \frac{G_b}{\rho} + \frac{G_k}{\rho} - \varepsilon \tag{5}$$

$$\overline{u_i} \frac{\partial \varepsilon}{\partial x_i} = \frac{1}{\rho} \frac{\partial}{\partial x_i} \left(\alpha_\varepsilon \mu_{eff} \frac{\partial \varepsilon}{\partial x_i} \right) + \frac{1}{\rho} C_{\varepsilon 1} \frac{\varepsilon}{k} \left(G_k + C_{\varepsilon 3} G_b \right) - C_{\varepsilon 2} \frac{\varepsilon^2}{k} - C_{\varepsilon 3}^* \tag{6}$$

Where,

$$C_{\varepsilon 3}^* = \frac{C_\mu \rho \eta^3 \left(1 - \frac{\eta}{\eta_o} \right)}{1 + \beta \eta^3} \frac{\varepsilon^2}{k}$$

$$G_b = \beta g \frac{\mu_t}{\mathrm{Pr}_t} \frac{\partial \overline{\theta}}{\partial x_i}$$

$$G_k = \mu_t S^2$$

$$\eta = \frac{Sk}{\varepsilon}$$

$$S = \sqrt{2 S_{ij} S_{ij}}$$

TABLE 1. EMPIRICAL MODEL CONSTANTS ADOPTED TO SOLVE GOVERNING MATHEMATICAL EQUATIONS

$C_{\varepsilon 1}$	$C_{\varepsilon 2}$	$C_{\varepsilon 3}$	C_μ	η_o	β	α_k	α_ε
1.42	1.68	$\tan\lvert v/u \rvert$	0.0845	4.38	0.012	Analytical	Formula

$$S_{ij} = \frac{1}{2}\left(\frac{\partial u_j}{\partial x_i} + \frac{\partial u_i}{\partial x_j}\right)$$

$$\beta = -\frac{1}{\rho}\left(\frac{\partial \rho}{\partial \theta}\right)_p$$

$$\mu_t = \rho C_\mu \frac{k^2}{\varepsilon}$$

The above transport equations for the conservation of mass (i.e. continuity Equation (1)), momentum (i.e. Equation (2)) and energy (i.e. Equation (3)) have considered air as an incompressible fluid [3, 22,26]. However, the effect of temperature on air density variation is pondered by employing Boussinesq approximation which treats density variation as a function of temperature change in the momentum equation as given:

$$\frac{\rho - \rho_n}{\rho_n} = -\beta(\theta - \theta_n)$$

The enhanced wall treatment is adopted in this model. The said scheme adopts a two layer model that works on different ranges of Reynolds number in free stream and near wall flow. In the case Reynolds number is high the turbulence model is used, else a two layer model is used to solve near wall flow [30].The said scheme resolves near-wall temperature and velocity gradients efficiently but a higher-resolution mesh is required, therefore, the near-wall mesh was refined accordingly. No slip boundary condition is employed at ground and building surfaces. Symmetry boundary is defined at the top and ground and other solid boundaries are defined with fixed temperature.

The physical model consists of seven street canyons and the depth for free stream flow was kept thrice as high as the street canon building height (Fig. 1). The number of canyons and the free stream depth were kept the maximum to give enough space for turbulence development. The mesh for the model is generated for AR1 and scaled to AR2 to 8 in Fluent code with the same number of elements for all ARs.

3. MODEL VALIDATION

The validation of the model is carried out by comparing the results of this model with those obtained from a wind tunnel experiment and two other numerical studies [22, 26, 31]. The normalized potential temperature and horizontal velocity of this model, the wind tunnel experiment and the two referred studies were all based on AR1. The results of this model were obtained at the centre line of the middle street canyon. Conversely, the results from this study, from referred wind tunnel experiment and the two numerical models were all based on a s-a (surface and air temperature difference) of 2K. Evidently, the temperature profiles obtained from our model have agreed very well with the wind tunnel data (Fig. 2). However, the comparison reflects that the deviations in velocity profiles are comparatively larger in particular above the canyon (Z/H>1.0). The validation and respective deviations in the results are illustrated in Fig. 2. The differences in the simulation results and wind tunnel data might have been a consequence of the differences in the simulation conditions and the experimental set-up. The roughness elements were not included in the simulation of our model while the referred experiment was carried out with such elements. Additionally, the modelled city blocks were arranged in a three-dimensional fashion in the wind-tunnel experiment while the model developed in this study was two-dimensional. However, despite the noted minor differences, overall results seem to have satisfactory followed the wind tunnel data.

4. RESULTS AND DISCUSSION

4.1 Results

The street canyon model was simulated with four different aspect ratios (i.e. AR1, 2, 4 and 8) each with four values for surface temperatures (i.e. 295, 297, 301 and 308 K) but only one value for ambient air temperature (i.e. 293K) is considered. However, different surfaces (i.e. ground,

leeward and windward wall) were defined with the same temperature in each different simulation case. Subsequently, all cases were simulated with the same u_a (i.e. 2.5m/s). The average air-temperature (area-weighted) within the target street canyon is normalized for different street-canyon heating situations as shown in Fig. 3. Obviously, there has been an increase in air-temperature with an increase in AR when $\Delta\theta_{s-a}$ was the highest (i.e. 16K). The highest temperatures were observed in AR8 street canyon in all the simulated cases (Fig. 3). Subsequently, the ascending order of resultant average temperature is AR1, 2, 4 and 8, respectively. This shows that the resultant temperature is directly proportional to the building aspect ratio. Results show that the highest $\Delta\theta_{AR}$ was around 3.3K (i.e. 1.1%) between the target street canyons of AR8 and 1 while average (area-weighted) temperatures in AR8, 4 and 2 were around 2.7, 2.3 and 0.1K higher than that in AR1 when $\Delta\theta_{s-a}$ was 16K. Fig. 4 shows the trend lines for the correlations between the resultant temperatures and building aspect ratios. Obviously, the

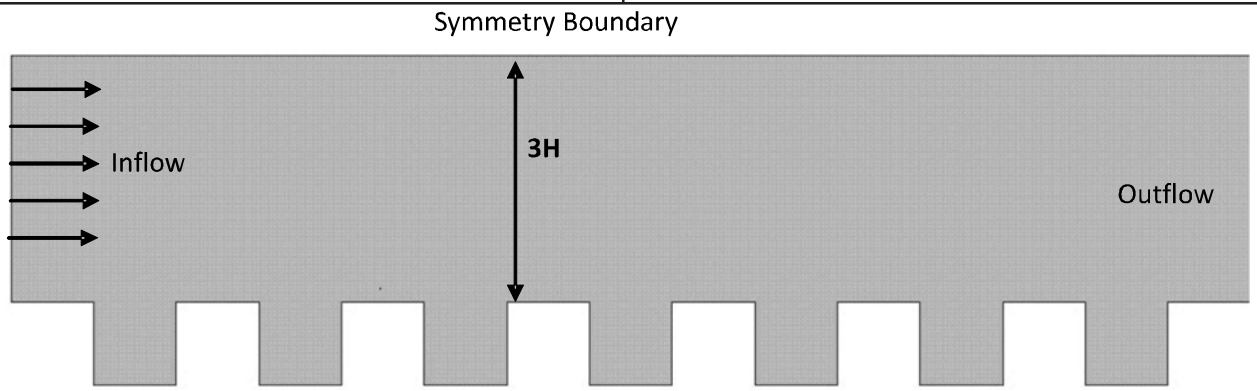

FIG. 1. SCHEMATIC DIAGRAM OF COMPUTATIONAL DOMAIN WITH BOUNDARY CONDITIONS

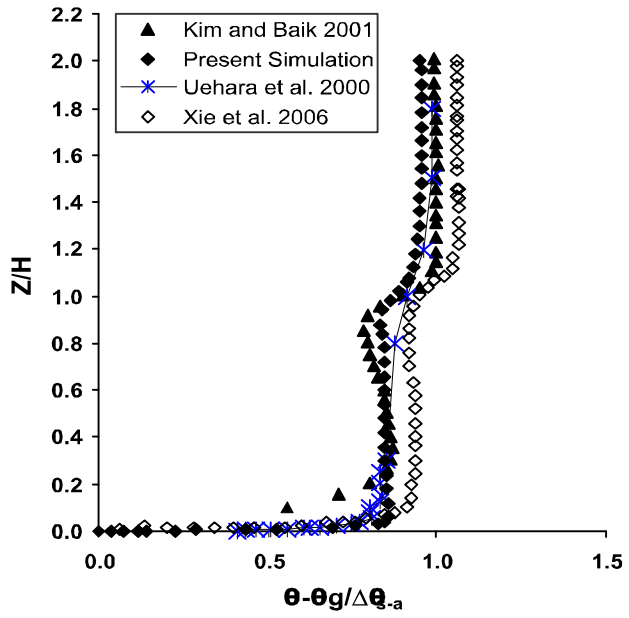

(a) HORIZONTAL VELOCITY

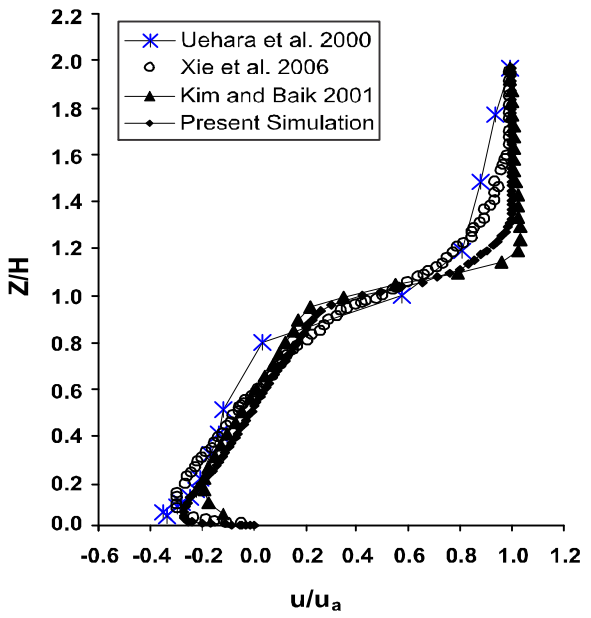

(b) POTENTIAL TEMPERATURE

FIG. 2. NORMALIZED HORIZONTAL VELOCITY AND POTENTIAL TEMPERATURE COMPARISON OF THIS STUDY, WIND TUNNEL EXPERIMENT AND TWO NUMERICAL STUDIES. THE RESULTS OF THIS STUDY WERE OBTAINED AT THE CENTRE LINE OF THE MIDDLE STREET CANYON

correlation between the resultant average temperatures and building aspect ratios is very strong (i.e. R^2 varies between 0.9 and 1.0). Consequently, the correlation was the strongest when $\Delta\theta_{s-a}$ was 2K (i.e. R^2=1.0) and less strong in the remaining cases. These results are very important as they illustrate temperature trends in the higher and lower aspect ratios during different heating situations. Memon, R.A., et. al. [3] showed that the temperature difference between the urban and rural areas would be the highest during the night-time and low or negative during the day-time or after-noon. The similar findings have been reported by many other studies [4, 32-33]. An analogy between the higher and lower aspect ratio street canyons and urban and rural areas could lead to important conclusions. Seemingly, the lower $\Delta\theta_{s-a}$ would represent day-time situation with uniform solar heating of air and street canyon surfaces. Subsequently, the higher $\Delta\theta_{s-a}$ would represent night-time situation as the temperature difference between air and street canyon surfaces would be due to their physical properties.

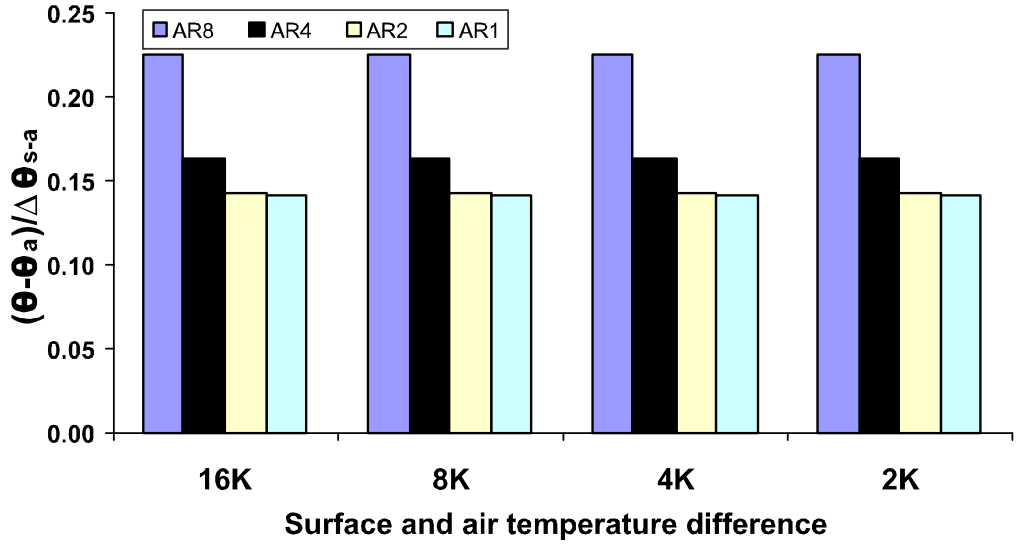

FIG. 3. NORMALIZED AVERAGE AIR-TEMPERATURE WITHIN THE TARGET STREET CANYON OF DIFFERENT BUILDING ASPECT RATIO

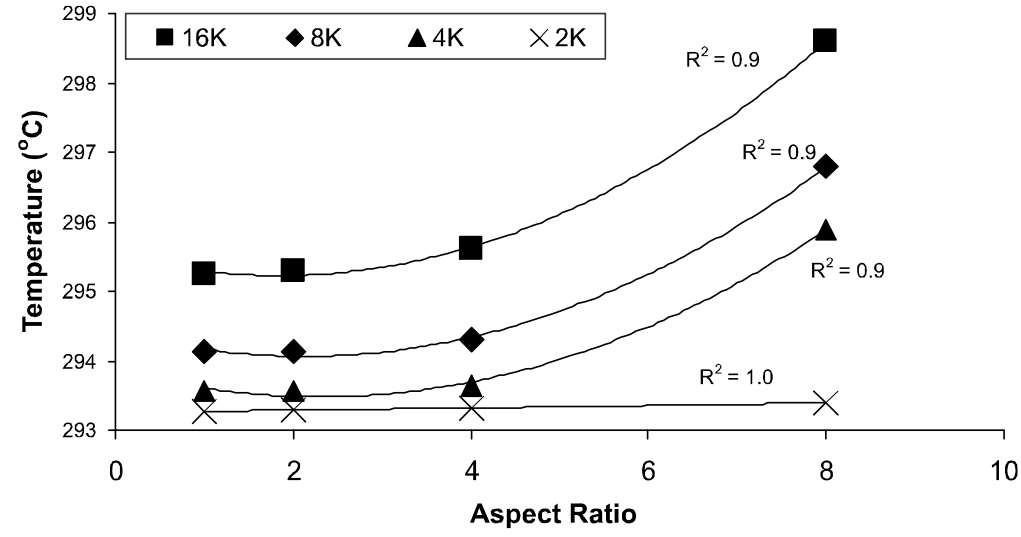

FIG. 4. A VIEW OF STRENGTH OF CORRELATION BETWEEN THE RESULTANT TEMPERATURES AND BUILDING ASPECT RATIOS

4.2 Discussion

Spatial isotherms and normalized velocity contours for different simulated cases are depicted in Fig. 5(a-b) for a detail analysis of the results with higher $\Delta\theta_{s-a}$ (i.e. 16K). It is evident that air-temperatures are higher in particular in the lower portion of the canyon in AR8. However, temperature reduces in the upper portion of the canyon. Seemingly, temperatures are comparatively higher on the leeward side of the canyon. A comparison with the velocity contours shows lower velocity throughout the canyon except some of the above portion of the canyon. Although possible impact of velocity magnitude on the temperature is clear it is not easy to recognize, possibly due to lower variation in velocity and temperature. However, it is clear that with high aspect ratio buildings the people living in the upper portion would be experiencing lower temperatures in particular on the windward side. Although one of the possible reasons of these higher temperatures would be higher heat flux due to larger wall surface area, the lower temperatures on one side of the walls shows that wind speed had an impact on the situation.

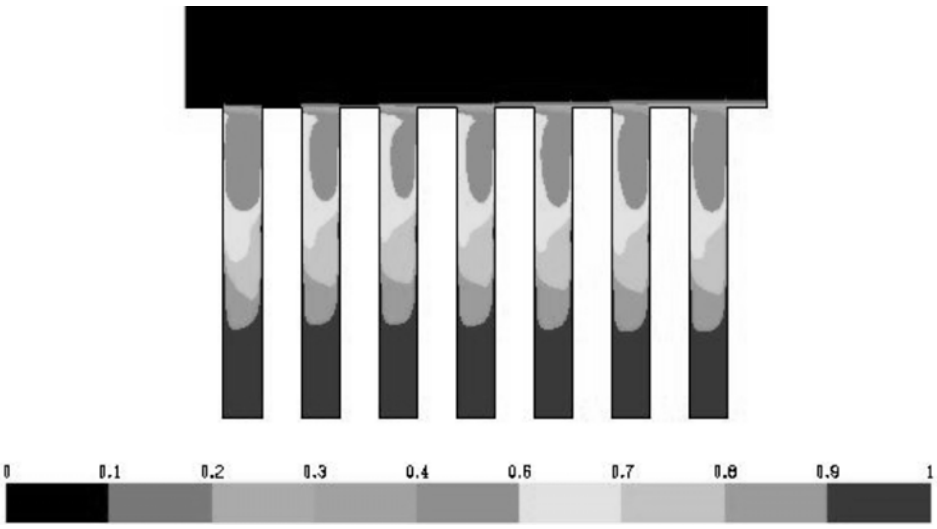

FIG. 5(A). AR 8: TEMPERATURE CONTOURS

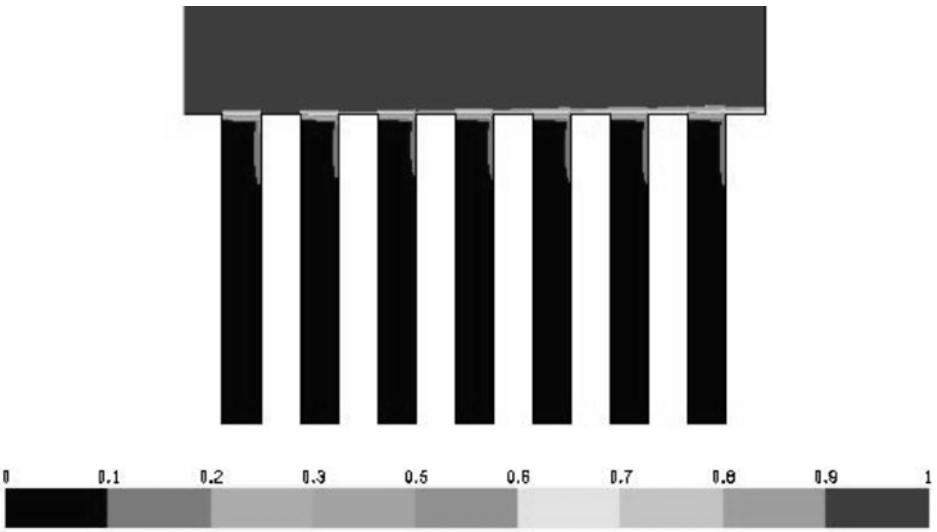

FIG. 5(B). AR 8: VELOCITY CONTOURS

A view of temperature and velocity contours in AR4 (Fig. 5(c-d)) shows that there is a clear difference between the temperature trends in AR8 and AR4. Evidently, only a little portion of the canyon ground is at higher temperature in AR4 as the rest of the canyon is comparatively cold. Apparently, the flow wind that enters from windward side looses the strength as it reaches the ground. It is also clear that temperatures are comparatively higher on the leeward side of the wall although the difference is insignificant. Evidently, the temperature distribution along the two walls is almost uniform within the canyon. A comparison with the velocity magnitude contours show that the impact of velocity magnitude is comparatively clearer in the case of AR4. Clearly, the velocity magnitude is lower on the higher temperature side (i.e. leeward side).

The temperature and velocity contours for AR2 are given in Fig. 5(e-f). Fig. 5(e) shows almost similar trends as the temperatures are comparatively higher on the leeward side. Conversely, temperatures are higher with the ground and lower above it. Also there is an un-noticeable portion for the highest range of the temperature (0-1.0) which shows that the temperatures in AR2 did not reach the upper limit observed in AR4 or AR8 street canyon.

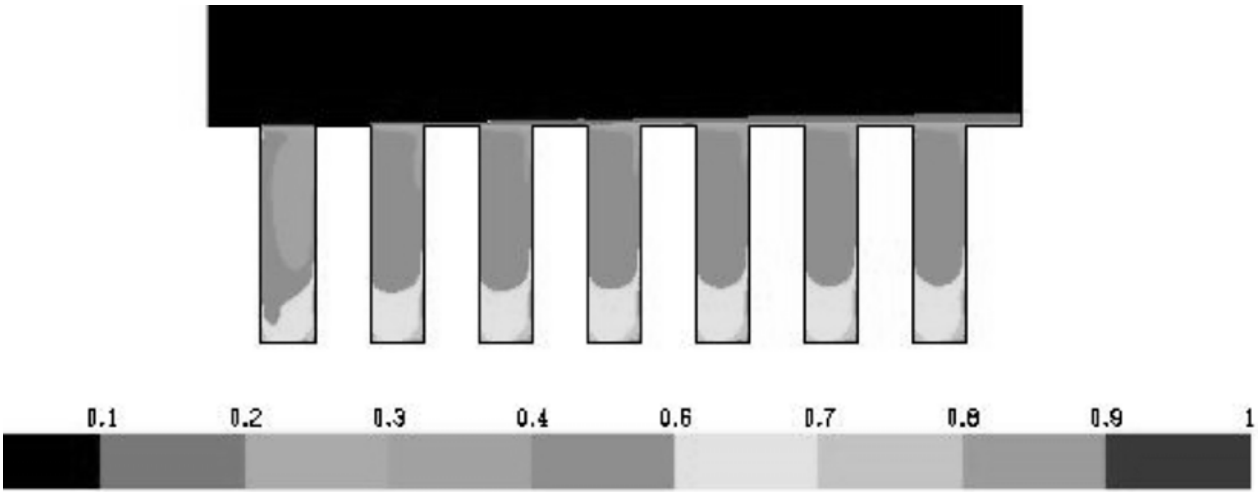

FIG. 5(C). AR4: TEMPERATURE CONTOURS

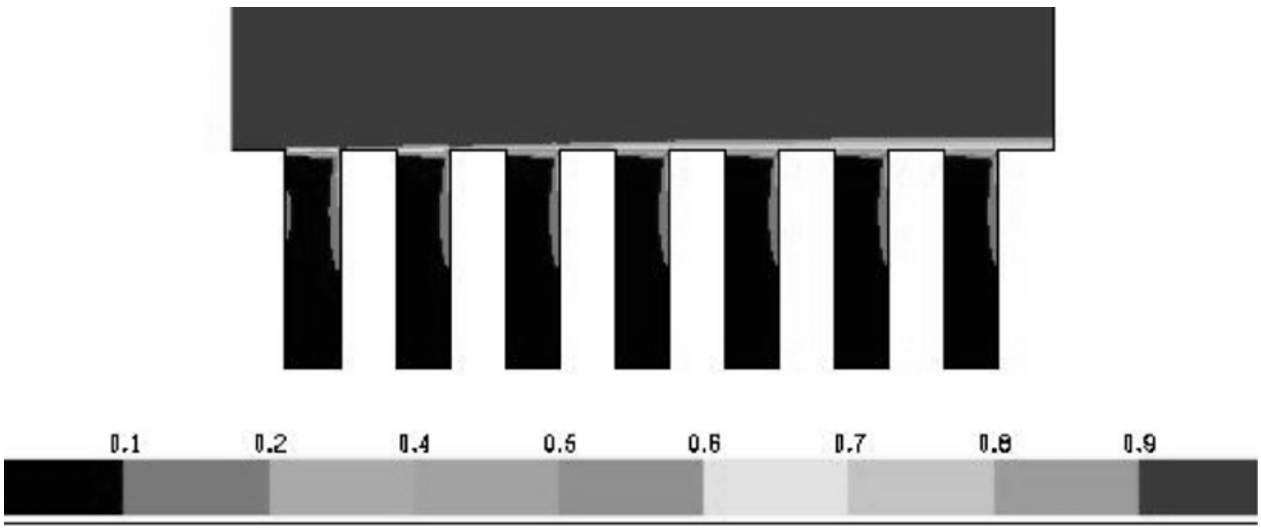

FIG. 5(D). AR4: VELOCITY CONTOURS

The resultant temperature and velocity contours in AR1 street canyon are shown in Fig. 5(g-h). Clearly, temperatures are lower on the windward side of the canyon. However, larger portion of the corner adjacent to the leeward side is at higher temperature. Conversely, velocity contours show lower velocity in the middle and with the corners of the canyon. However, the middle of the canyon, that covered by the lower velocity, is accompanied with a higher temperature (Fig. 5(g)). Apparently, the lower temperature in the middle of the canyon as compared to the corners is caused by an uneven velocity distribution.

A common point observed in all the cases is that the lower temperature contour enters into the canyon from the windward side. Notably, the strong wind of higher speed enters in the canyon from the windward side. This hints that higher velocity has been the reason of lower temperatures on the windward side. A comparison shows that the temperature variation with respect to velocity is clearer above street canyon. Clearly, three different ranges of temperature contours above street canyon starts with the higher temperature adjacent with the canyon and ends with the lowest temperature. Conversely, four different

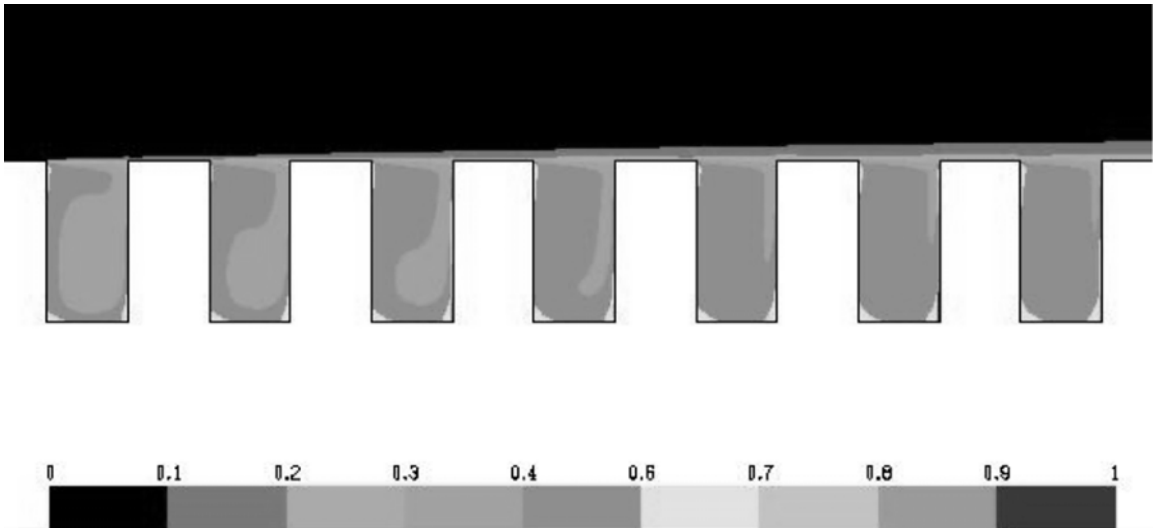

FIG. 5(E). AR2: TEMPERATURE CONTOURS

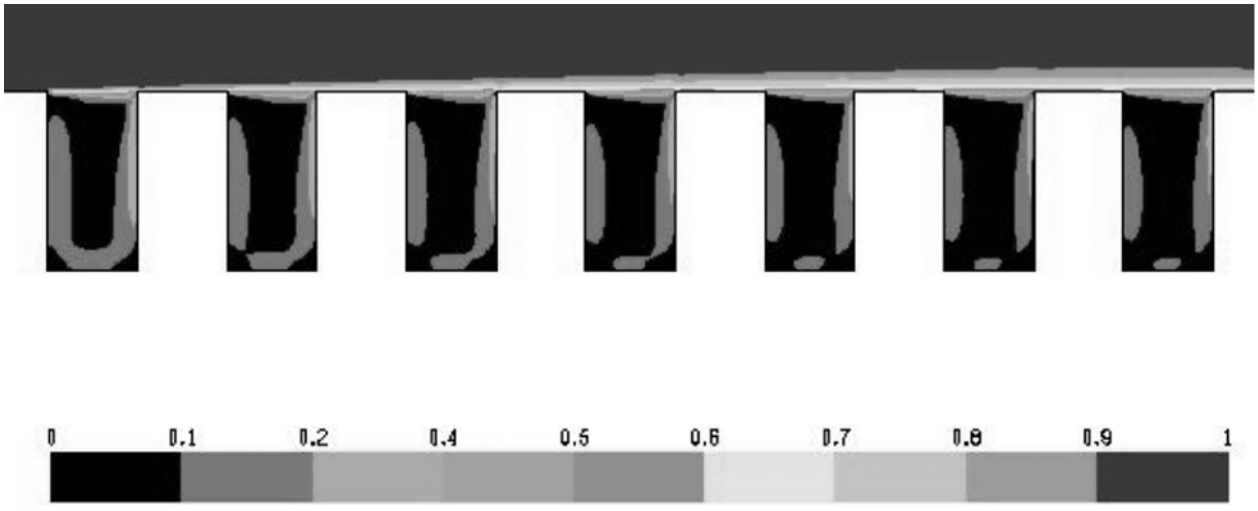

FIG. 5(F). AR2: VELOCITY CONTOURS

ranges of velocity could easily be seen adjacent with the top of the canyon starting with the lowest velocity and reaching the highest.

5. CONCLUSIONS

A two dimensional k-ε turbulence model with RNG closure scheme was adopted to assess the effects of street-canyon heating. It was found that the temperature difference in the higher and lower AR street canyon was increased with an increase in the surface and air temperature difference. Additionally, air-temperature increases with an increase in street canyon aspect ratio. Apparently, lower velocity due to higher building aspect ratio was a main reason of higher heating. Additionally, heating was comparatively higher on the leeward side of the canyon in higher AR street canyons. Notably, the variation in air-temperatures and velocity magnitude was rapid and clearer over the street canyon. It was also concluded that the wind that enters from windward side reduces the temperature on that side but looses strength as the flow cross over the ground. The results of this study could be helpful to civil engineers and city planners as the results show the

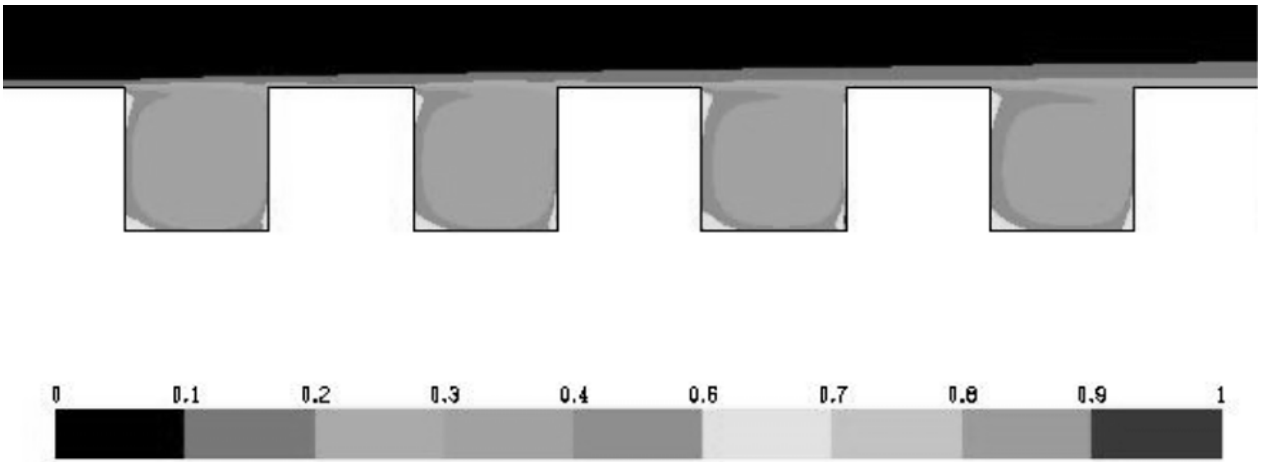

FIG. 5(G). AR1: TEMPERATURE CONOURS

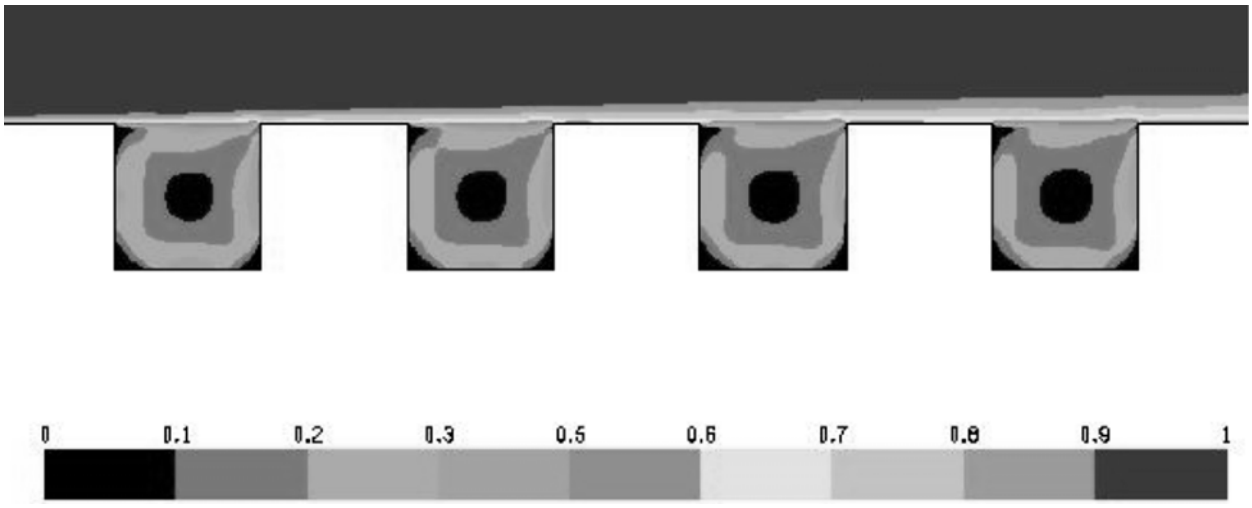

FIG. 5(H). AR1: VELOCITY CONTOURS

FIG. 5. TEMPERATURE AND VELOCITY CONTOURS WITHIN AR8 (A-B), AR4 (C-D), AR2 (E-F) AND AR1 (G-H).

difference in temperature with respect to aspect ratio and wind speed. The city planners can design an optimum aspect ratio that must assure minimum temperature rise keeping in view the ambient wind speed and population density of an area. It was also revealed that the people living in the upper portion of high aspect ratio street canyon would be experiencing lower temperatures in particular on the windward side.

6. NOMENCLATURE

AR	Aspect Ratio
H	Street canyon height (m)
W	Street canyon width (m)
G_b	Turbulence kinetic energy production due to buoyancy ($kgm^{-1}s^{-3}$)
X/W	Spatial co-ordinate in horizontal direction divided with street canyon width
$\bar{u}_i$	Mean stream-wise (μ) and vertical (υ) velocity components (ms^{-1})
u_a	Horizontal inflow wind speed (ms^{-1})
ε	Dissipation rate of turbulent kinetic energy ($m^2 s^{-3}$)
S_{ij}	Mean rate of strain tensor (1/s)
g	Ground level temperature (K)
$\Delta\theta_{ARi}$	Average air-temperature difference between the target street canyons of high and low ARs (K)
g	Acceleration due to gravity (m/s^2)
p	Fluid pressure (Pascal)
u_i	Velocity components (m/s)
G_k	Turbulence kinetic energy production due to mean velocity gradient ($kgm^{-1} s^{-3}$)
Z/H	Spatial coordinate in Z direction non-dimensionalized by street canyon height
Re_H	Reynolds number (based on street canyon height) = $u_a H/\nu$
R_b	Bulk Richardson number $\frac{gH(\theta_a - \theta_g)}{\theta_a u_a^2}$
k	Turbulent kinetic energy ($m^2 s^{-2}$)
$\bar{\theta}$	Mean temperature
θ_a	Ambient air-temperature (K)
$\Delta\theta_{s-a}$	Difference between the surface and ambient air-temperature (K)

ACKNOWLEDGEMENT

This work was carried out with the financial support provided by the University Research Committee of the University of Hong Kong. The author is grateful to the Department of Mechanical Engineering, Mehran University of Engineering and Technology, Jamshoro, Pakistan, for providing necessary facilities to write this paper.

REFERENCES

[1] Unger, J., Sumeghy, Z., and Zoboki, J., "Temperature Cross-Section Features in an Urban Area", Atmospheric Research, Volume 58, pp. 117-127, 2001.

[2] Memon, R.A., Leung, D.Y.C., and Liu, C.H., "A Review on the Generation, Determination and Mitigation of Urban Heat Island", Journal of Environmental Sciences, Volume 20, pp. 120-128, 2008.

[3] Memon, R.A., Leung, D.Y.C., and Liu, C.H., "Effects of Building Aspect Ratio and Wind Speed on Air-Temperatures in Urban-Like Street Canyons", Building and Environment, Volume 45, pp. 176-188, 2010.

[4] Hafner, J., and Kidder, S.Q., "Urban Heat Island Modelling in Conjunction with Satellite-Derived Surface/ Soil Parameters", Journal of Applied Meteorology, Volume 38, pp. 448-465, 1999.

[5] Konopacki, S., and Akbari, H., "Energy Savings for Heat Island Reduction Strategies in Chicago and Houston (Including Updates for Baton Rouge, Sacramento, and Salt Lake City)", Draft Final Report, LBNL-49638, University of California, Berkeley, 2002.

[6] Rosenfeld, A.H., Akbari, H., Romm, J.J., and Pomerantz, M., "Cool Communities: Strategies for Heat Island Mitigation and Smog Reduction", Energy and Buildings, Volume 28, pp. 51-62, 1998.

[7] Changnon, S.A., Kunkel, K.E., and Reinke, B.C., "Impacts and Responses to the 1995 Heat Wave: A Call to Action", Bulletin of the American Meteorological Society, Volume 77, pp. 1497-505, 1996.

[8] Memon, R.A., Leung, D.Y.C., and Liu, C.H., "A Review on the Generation, Determination and Mitigation of Urban Heat Island", Journal of Environmental Sciences, Volume 20, pp.120-128, 2008.

[9] Lemonsu, A., and Masson, V., "Simulation of a Summer Urban Breeze Over Paris, Boundary Layer Meteorology", Volume 104, pp. 463-490, 2002.

[10] Ashie, Y., Thanh, V.C., and Asaeda, T., "Building Canopy Model for the Analysis of Urban Climate", Journal of Wind Engineering and Industrial Aerodynamics", Volume 81, pp. 237-248, 1999.

[11] Dupont, S., Otte, T., and Ching, J.K.S., "Simulation of Meteorological Fields within and Above Urban and Rural Canopies with a Mesoscale Model (MM5)", Boundary Layer Meteorology, Volume 113, pp. 111-158, 2004.

[12] Huang, H., Ooka, R., and Kato, S., "Urban Thermal Environment Measurements and Numerical Simulation for an Actual Complex Urban Area Covering a Large District Heating and Cooling System in Summer", Atmospheric Environment, Volume 39, pp. 6362-6375, 2005.

[13] Kato, S., and Yamaguchi, Y., "Analysis of Urban Heat Island Effect Using ASTER and ETM + Data: Separation of Anthropogenic Heat Discharge and Natural Heat Radiation from Sensible Heat Flux", Remote Sensing of Environment, Volume 99, pp. 45-54, 2005.

[14] Masson, V., "A Physically Based Scheme for the Urban Energy Budget in Atmospheric Models", Boundary Layer Meteorology, Volume 94, pp. 357-397, 2000.

[15] Masson, V., Grimmond, C.S.B., and Oke, T.R., "Evaluation of the Town Energy Balance (TEB) Scheme with Direct Measurements from Dry Districts in Two Cities", Journal of Applied Meteorology, Volume 41, pp. 1011-1026, 2002.

[16] Takahashi, K., Yoshida, H., Tanaka, Y., Aotake, N., and Wang, F., "Measurement of Thermal Environment in Kyoto City and its Prediction by CFD Simulation", Energy and Buildings, Volume 36, pp. 771-779, 2004.

[17] Yamada, T., "Building and Terrain Effects in a Mesoscale Model", 11th Conference on Air Pollution Meteorology, Long Beach California, pp. 215-220, New Mexico 9-14 January, 2000.

[18] Eliasson, I., and Offerle, B., "Wind Fields and Turbulence Statistics in an Urban Street Canyon", Atmospheric Environment, Volume 40, pp. 1-16, 2006.

[19] Li, X., Liu, C.H., and Leung, D.Y.C., "Development of a K-ε Model for the Determination of Air Exchange Rates for the Street Canyons", Atmospheric Environment, Volume 39, pp. 7285-7296, 2005.

[20] Liu, C.H., Leung, D.Y.C., and Barth, M.C., "On the Prediction of Air and Pollutant Exchange Rates in Street Canyons of Different Aspect Ratios Using Large-Eddy Simulation", Atmospheric Environment, Volume 39, pp. 1567-1574, 2005.

[21] Xia, J.Y., and Leung, D.Y.C., "Pollutant Dispersion in Urban Street Canopies, Atmospheric Environment", Volume 35, pp. 2033-2043, 2001.

[22] Xie, X., Huang, Z., and Wang, J.S., "The Impact of Urban Street Layout on Local Atmospheric Environment", Building and Environment, Volume 41, pp. 1352-1363, 2006.

[23] Xie, X., Liu, C.H., Leung, D.Y.C., and Leung, M.K.H., "Impact of Building Facades and Ground Heating on Wind Flow and Pollutant Transport in Street Canyons", Atmospheric Environment, Volume 41, pp. 9030-9049, 2007.

[24] Kim, J.J., and Baik, J.J., "Urban Street-Canyon Flows with Ground Heating", Atmospheric Environment, Volume 35, pp. 3395-3404, 2001.

[25] Sini, J.F., and Anquetin, S., "Pollution Dispersion and Thermal Effects in Urban Street Canyon", Atmospheric Environment, Volume 30, 2659-2677, 1996.

[26] Xie, X., Huang, Z., Wang, J.S., and Xie, Z., "The Impact of Solar Radiation and Street Layout on Pollutant Dispersion in Street Canyon", Building and Environment, Volume 40, pp. 201-212, 2005.

[27] Xie, X., Liu, C.H., Leung, D.Y.C., and Leung, M.K.H., "Characteristics of Air Exchange in a Street Canyon with Ground Heating", Atmospheric Environment Volume 40, pp. 6396-6409, 2006.

[28] Memon, R.A., Leung, D.Y.C., and Liu, C.H., "An Investigation of Urban Heat Island Intensity (UHII) as an Indicator of Urban Heating", Atmospheric Research, Volume 94, pp. 491-500, 2010.

[29] Chan, T.L., Dong, G., Leung, C.W., Cheung, C.S., and Hung, W.T., "Validation of a Two-Dimensional Pollutant Dispersion Model in an Isolated Street Canyon", Atmospheric Environment, Volume 36, pp. 861-72, 2002.

[30] Fluent User Guide Version 6.2.1, 2005.

[31] Uehara, K., Murakami, S., Oikawa, S., and Wakamatsu, S., "Wind Tunnel Experiments on How Thermal Stratification Affects Flow in and Above Urban Street Canyons", Atmospheric Environment, Volume 34, pp. 1553-1562, 2000.

[32] Montavez, J.P., Rodriguez, A., and Jimenez, J.I., "A Study of the Urban Heat Island of Granada", International Journal of Climatology, Volume 20, pp. 899-911, 2000.

[33] Memon R.A., Leung, D.Y.C., Liu, C.H., and Leung, M.K.H., "Urban Heat Island and its Effect on the Cooling and Heating Demands in Urban and Suburban Areas of Hong Kong", Theoretical and Applied Climatology, Volume 10, 2010.DOI: http://www.springerlink.com/content/c4v540546642u850/